Journal of Histochemistry & Cytochemistry 59(10) 918–931

DOI: 10.1369/0022155411417309
http://jhc.sagepub.com
SAGE

Genotypic and Phenotypic Differences between Nodal and Extranodal Diffuse Large B-Cell Lymphomas

Salah A. Al-Humood, Aisha S. Al-Qallaf, Salem H. AlShemmari, Issam M. Francis, Thamradeen A. Junaid, Rajaa A. Marouf, and Fahd Al-Mulla
Department of Pathology (SAA,ASA,IAF,TAJ,RAM,FA) and Department of Medicine, Faculty of Medicine, Kuwait University, Safat, Kuwait (SHA)

Summary

Diffuse large B-cell lymphoma (DLBCL) is a heterogeneous group of diseases that have diverse clinical, pathological, and biological features. Here, it is shown that primary nodal and extranodal DLBCLs differ genomically and phenotypically. Using conventional comparative genomic hybridization (CGH), the authors assessed the chromosomal aberrations in 18 nodal, 13 extranodal, and 5 mixed DLBCLs. The results demonstrate significantly distinct chromosomal aberrations exemplified by gains of chromosomal arms 1p, 7p, 12q24.21-12q24.31, and 22q and chromosome X and loss of chromosome 4, 6q, and 18q22.3-23 in extranodal compared with nodal DLBCLs. Nodal DLBCLs showed an increased tendency for 18q amplification and BCL2 protein overexpression compared with extranodal and mixed tumors. Using a panel of five antibodies against GCET1, MUM1, CD10, BCL6, and FOXP1 proteins to subclassify DLBCLs according to the recent Choi algorithm, the authors showed that the genomic profiles observed between the nodal and extranodal DLBCLs were not due to the different proportions of GCB vs ABC in the two groups. Further delineation of these genomic differences was illuminated by the use of high-resolution 21K BAC array CGH performed on 12 independent new cases of extranodal DLBCL. The authors demonstrated for the first time a novel genome and proteome-based signatures that may differentiate the two lymphoma types. (J Histochem Cytochem 59:918–931, 2011)

Keywords

diffuse large B-cell lymphoma (DLBCL), nodal DLBCL, extranodal DLBCL, comparative genomic hybridization (CGH), BCL2, microarray CGH, Choi classification, ABC, GCB, GCET1, MUM1, CD10, BCL6, FOXP1

Non-Hodgkin's lymphoma (NHL) is a heterogeneous group of diseases that have different morphological, immunological, cytogenetic, and molecular features. Diffuse large B-cell lymphoma (DLBCL) is the most common subtype of NHL in adults worldwide, accounting for 30% to 40% of lymphoid neoplasms. Recent statistical data from Kuwait also indicate that DLBCL is the most common form of NHL. It is the third most common malignant disease among Kuwaiti women after cancer of the breast and lungs and the fifth most common among Kuwaiti men (Ameen et al. 2010). The World Health Organization (WHO) published a report on the classification of hematological malignancies and proposed to classify DLBCL as a separate clinicopathological entity in its classification of NHL. DLBCL is the largest category of aggressive lymphoma and is regarded by many pathologists and oncologists to be a heterogeneous group of disorders that requires further subclassification. This view was based on the fact that morphological and immunophenotypic approaches to the diagnosis of this disease are insufficient to predict

Received for publication September 14, 2010; accepted June 2, 2011.

Supplementary material for this article is available on the *Journal of Histochemistry & Cytochemistry* Web site at http://jhc.sagepub.com/supplemental.

Corresponding Author:
Fahd Al-Mulla, Department of Pathology, Molecular Pathology Unit, Faculty of Medicine, Kuwait University, P. O. Box: 24923, Safat 13110, Kuwait.
E-mail: fahd@al-mulla.org

patient outcome in a particular case, and although histologically similar, cells behave differently in different patients.

Several studies have shown that DLBCLs are associated with a wide range of recurrent chromosomal abnormalities and molecular genetic defects. Gene expression profiling has identified three major subgroups of DLBCLs: germinal center B-cell–like DLBCL (GCB-DLBCL), activated B-cell–like DLBCL (ABC-DLBCL), and primary mediastinal DLBCL (PMBCL) (Alizadeh et al. 2000; Savage et al. 2003; Rosenwald et al. 2002; Rosenwald and Staudt 2003; Wright et al. 2003; Bea et al. 2005; Lawrie et al. 2007; Choi et al. 2009). These three subgroups of DLBCL are associated with a widely disparate clinical outcome with 5-year survival rates of 59%, 30%, and 64% in patients with GCB-DLBCL, ABC-DLBCL, and PMBCL, respectively (Alizadeh et al. 2000). At the DNA level, few studies have profiled chromosomal aberrations in different subgroups of DLBCL. For example, Tagawa et al. (2005) identified distinct chromosomal aberrations in ABC ($CD5^+$), GCB ($CD5^-CD10^+$), and mixed ABC and GCB ($CD5^-CD10^-$) subgroups of nodal DLBCL. In their study, distinct chromosomal aberrations between the ABC and GCB group were evident and the CD5(+) DLBCL appears to show similar genomic imbalances to the ABC group (Tagawa et al. 2005). However, to the best of our knowledge, there is currently no study in the scientific literature comparing the chromosomal aberrations of nodal and extranodal DLBCL. We think such a comparison is important for at least two reasons. First, if distinct aberrations were identified between the two subgroups of DLBCL, this may suggest diverged disease entities and therefore may also explain the significant multifaceted heterogeneity observed in DLBCL patients. Second, in the age of personalized medicine, the identification of a precise genetic signature may aid in the delivery of appropriate/personalized therapeutic intervention.

Using metaphase-based comparative genomic hybridization (CGH) and confirmation of the data in an additional and separate cohort of extranodal DLBCL, this study tests the hypothesis that nodal and extranodal DLBCL are clonally distinct B-cell diseases.

Materials and Methods

Patients and Tumor Specimens

A total number of 45 patients was selected to be included in the study. The patients were diagnosed between 1988 and 2001 and were identified from the files of the departments of pathology from five general hospitals. Twenty-three (51%) patients had DLBCL disease limited to nodal sites and 17 (37.7%) patients had the disease limited to extranodal sites. Five patients had mixed nodal with extranodal involvement in at least one site. A separate cohort included 12 patients with extranodal DLBCL (8 patients with head and oral tumors, 2 gastrointestinal tumors, 1 bone tumor, and 1 thyroid-localized DLBCL) diagnosed and staged at the Kuwait Cancer Control Center (KCCC). All patients were staged in the KCCC by bone marrow examination and computed tomography scan of the chest, abdomen, and pelvis. No patient received chemotherapy prior to obtaining the biopsies for our study.

Histopathology

Tissues were fixed in 10% formalin and embedded in paraffin. Sections (5 μM thick) were stained with hematoxylin and eosin (H&E). All patients were reviewed by 4 experienced pathologists, and the diagnosis of DLBCL was confirmed according to the 2008 WHO lymphoma classification.

Immunohistochemical Staining Studies

Immunohistochemical staining using anti-CD20, -CD79α, -CD3, -CD5, and -BCL2 (all from Dako, Glostrup, Denmark) were manually performed on all patients. For Choi classification, parallel sections of each patient were stained for GCET1 (Abcam, SF), MUM1 (Abcam, SF), CD10 (NCL-L-CD10-270, Novocastra, Newcastle, UK), BCL6 (Dako, Denmark), and FOXP1 (Abcam, SF) proteins. In all histochemical experiments, the sections were deparaffinized thrice with xylene, dehydrated twice with 100% and 95% alcohol, dehydrated once with 70% alcohol for a minimum of 3 min each, washed with distilled water, blocked with 3% hydrogen peroxide for 10 min, and treated with heat-induced epitope retrieval solution in a stainless steel pressure cooker for 8 min. Then the sections were incubated with the primary antibody for 1 hr, biotinylated secondary antibody (Vector Laboratories, Burlingame, California) for 30 min, ABC reagent (Vector Laboratories, Burlingame, California) for 30 min, and DAB until the desired stain intensity developed. The sections were counterstained with hematoxylin; sequentially dehydrated with 70% alcohol once and with 95% alcohol, 100% alcohol, and xylene twice; and mounted. The proportion of positively stained cells was estimated on sections from each tissue biopsy based on positively stained area and the intensity of staining.

Fluorescence In Situ Hybridization (FISH)

The method for FISH analysis has been optimized and manually performed. Sections were deparaffinized thrice with xylene and then rehydrated to distilled water after passing through 100%, 90%, and 70% alcohol for 1 min each. The sections were incubated in a couplin jar containing 40 ml of 1× phosphate-buffered saline (PBS), 400 μL of proteinase-K (20 mg/ml), and 200 μL of 10% sodium dodecyl sulfate (SDS) at 55C for 9 min or until the tissue is

properly digested. The slides were then washed thrice with 1× PBS for 5 min each, followed by treatment with 0.1 mg/ml 2× SSC RNase A (20 mg/ml) at 37C for 1 hr and washing with 2× SSC three times for 5 min each. The dehydrated sections were denatured in 70% formamide/2× SSC at 73C for 5 min. After dehydrating with ice-cold 70%, 90%, and 100% alcohol for 3 min each, the slides were air dried at 37C. The Probe mixture (PathVysion, Abbott Molecular, Illinois) was prepared by adding 1 μL of LSI probe to 7 μL of LSI/WCP hybridization buffer and 2 μL of purified water. The probe was denatured at 73C for 5 min and applied to the target, the cover slip was sealed, and the slides were left overnight in a prewarmed, humidified Hybaid Omnislide (ThermoFisher Scientific, Massachusetts) for hybridization. The next day the slides were washed in 50% formamide for 10 min, 2× SSC for 10 min, and 2× SSC/0.1% Tween-20 for 5 min at 46C, dehydrated, and counterstained with DAPI.

DNA Extraction From Tissue Specimens

Before the start of DNA extraction, H&E-stained tissue sections were examined by four pathologists. The pathologists scored the percentage of tumor area to avoid false-negative results. Tumors representing more than 50% of the total tissue were selected for DNA extraction. DNA was extracted from 4 × 20 μm paraffin-embedded tissue sections cut into sterile 1.5-ml Eppendorf tubes. Sections were deparaffinized three times with xylene for 30 min at room temperature and dehydrated three times with 100% alcohol. The tissue pellet was finally washed with 70% alcohol and dried under vacuum. To the tissue pellet, 500 μl of cell lysis solution (Puregene, Gentra Systems, Qiagen, Hilden, Germany) was added along with 20 μL of proteinase K (20 mg/ml). The samples were incubated at 56C for 5–6 days until completely digested. To the digested sample, 4 μl of RNAase A (4 mg/mL) was added and incubated at 37C for 30 min. Two hundred μl of protein precipitation solution (Puregene, Qiagen, Hilden, Germany) was added to precipitate proteins by centrifugation at 14,000 × g for 5 min. The supernatant was added to an Eppendorf tube containing 600 μl of isopropanol and the mixture was inverted 50 times to precipitate the DNA at 14,000 × g for 4 min.

The DNA pellet was then washed with 70% alcohol, dried, and dissolved in 60–70 μl of DNA hydration buffer (Puregene). The concentration of the DNA was measured spectrophotometrically. The quality of DNA extraction was assessed using agarose gel electrophoresis.

DNA was extracted from 36 patients, and the quality of the extracted DNA was confirmed by running 5 μL alongside 100 bp DNA ladder on a 1% agarose gel stained with ethidium bromide. Samples showing high-molecular-weight DNA with background smearing were selected for CGH experiments. Normal DNA was prepared from a healthy normal male and female for CGH experiments using the above procedure.

Conventional Metaphase and Microarray-Based CGH

Metaphase CGH was performed and quantitated following previously published protocol (Al-Mulla et al. 2006). For array CGH (aCGH), DNA was extracted from five sections of 20 μM formalin-fixed paraffin-embedded (FFPE) tissue using the Gentra Puregene Tissue Kit (Qiagen, Hilden, Germany) according to the manufacturer's protocol. Two thousand ng of FFPE DNA and pooled sex-matched reference DNA (Promega, WI) were sonicated in a water bath (Elmasonic, Singen, Germany) for 30 sec. Chemical labeling was carried out using the universal linkage system (ULS) Cy3 and Cy5 (Kreatech, Amsterdam, Netherlands) dyes for 1 hr at 85C. The sample DNA was labeled with Cy5 and the reference DNA with Cy3 in each patient. The unreacted Cy-ULS was removed using KREApure columns (Kreatech, Amsterdam, Netherlands). The degree of labeling (DOL) was calculated by using the Nanodrop ND 1000 Spectrophotometer readings using the DOL calculator according to the ULS array CGH labeling kit for BAC arrays user guide (version 1.0). The Cy5-labeled tumor and matching Cy3-labeled reference samples were combined and concentrated by precipitation with 50 μl of Cot I DNA (Invitrogen, CA), 90 μl of 0.3 M sodium acetate (Sigma, St. Louis, MO), and 225 μl of ice-cold ethanol. The pellet obtained after centrifugation was resuspended in 5.2 μl of KREAblock buffer (Kreatech, Amsterdam, Netherlands), 10.8 μl of 10% SDS solution (Sigma, St. Louis, Missouri), and 8 μl of Yeast tRNA (Invitrogen, California) at 50 μg/μl and incubated at room temperature for 10 min. Twenty-six μl of KREAhyb-CGH (Kreatech, Amsterdam, Netherlands) was added and the hybridization mix was incubated at 70C for 15 min, which was followed by a 30-min incubation at 37C. The entire probe was added to the Ultra High Resolution Pangenomic Tiling 21K BAC Arrays (Array Genomics, Paris, France) and hybridized in a hybridization chamber (Corning, NY) at 42C for 16 hr. After hybridization, the slides were disassembled by immersing them in Wash Buffer I (0.1× SSC, 0.1% SDS) at 50C. The slides were then washed twice for 45 sec each in Wash Buffer I at 50C and twice for 45 sec each in Wash Buffer II (0.1× SSC) at 50C. The slides were quickly plunged into Wash Buffer II at room temperature followed by a quick dip in 100% ethanol. The slides were dried by spinning them down in a 50-ml conical tube for 15 sec. To minimize the impact of environmental factors on the signal intensities, the slides were scanned immediately on an Agilent Microarray scanner (Agilent Technologies, CA) at 5 μm resolution according to the Agilent G2565AA and Agilent G2565BA Microarray Scanner System with SureScan Technology User Guide (version 7.0). Images were

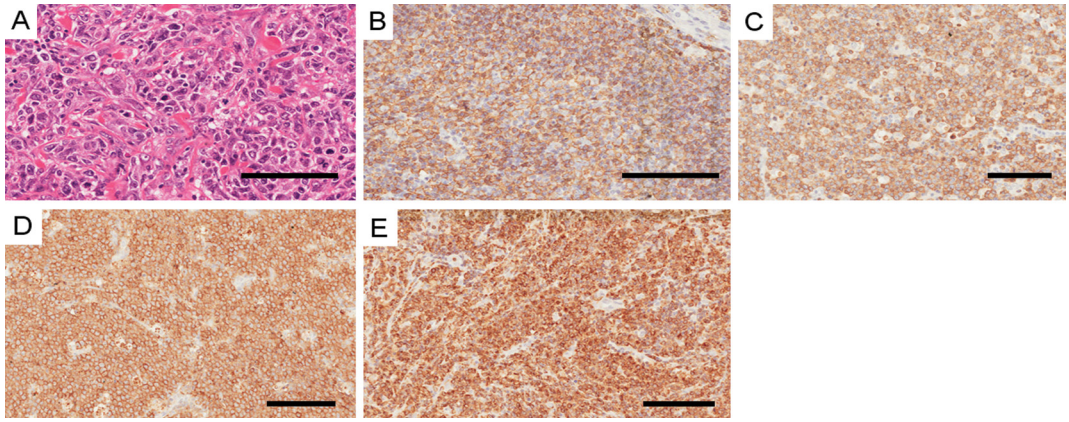

Figure 1. Phenotypic characteristics of diffuse large B-cell lymphoma (DLBCL). (A) Centroblastic variant of a DLBCL case (hematoxylin and eosin–stained paraffin section). (B) Immunohistochemical staining for CD20. (C) CD79α. (D) CD10. (E) BCL2 proteins in neoplastic cells. Bars = 100 μm.

annotated, normalized, and analyzed using Biodiscovery Imagene and Nexus V5.0 software (Biodiscovery, California).

Polymerase Chain Reaction

PCR amplification was performed using various primer sets for clonality demonstration, including VHCon-JH, VH26-JH6, FR1fVH1, FR1fVH2, FR1fVH3-JH, FR1fVH4, FR1fVH5, FR1fVH6-JH, and MC8C-JH18 for t(14;18) to improve the sensitivity of monoclonality detection.

For PCR, 1 μL of extracted DNA (400 ng) and 1.5 μL each of forward and reverse primers (10 pmol/μL) were added to the PCR master mix (ABgene, (ThermoFisher Scientific, Massachusetts) to obtain a final reaction volume of 50 μL. The PCR master mix consisted of 1.25 U of *Taq* DNA polymerase, 75 mM Tris-HCl (pH 8.8 at 25C), 20 mM (NH4)2SO4, 2.5 mM MgCl2, 0.01% (v/v) Tween 20, and 0.2 mM each of dATP, dCTP, dGTP, and dTTP. Each reaction included one tube of normal DNA and a DLBCL case as polyclonal and monoclonal controls, respectively. The PCR conditions varied for different primers. The VHCon/JH (JH3, JH6, JH1245) assay was an adequate initial primer set. Negative samples were further evaluated with primer sets (1) VH26-JH6 (2) Fr1fVH1, FR1fVH2, FR1fVH3-JH (3) FR1fVH4, FR1fVH5, FR1fVH6- JH (4) BCL-2-JH for t(14;18), and each step was carried out using negative samples from the previous set. The PCR products were visualized on 8% polyacrylamide gels and the data digitally recorded.

Statistical Analysis

The distribution of the number of CGH alterations in the two subgroups was compared using the Student's *t*-test. The Fisher's exact and χ^2 tests were used to compare contingency tables. Probabilities of <0.05 were considered statistically significant. The statistical analyses were performed using the SPSS software version 17.

Results

Clinical and Molecular Characterization of DLBCL

Forty-five cases of DLBCL were examined in this study. All patients showed a diffuse and monomorphic proliferation of large, morphologically centroblastic cells that had round nuclei with vesicular chromatin and small distinct nucleoli (Figure 1A). Clonal analysis using PCR was performed on 36 cases that were suitable for DNA amplification. Monoclonality was demonstrated in 34 patients of the 36 patients (94.4%) using multiple primer sets.

Thirty-four patients (75.6%) were males and 11 (24.4%) were females. The mean age was 46.3 years and the median was 46 years. The age range was between 6 and 89 years.

Twenty-three (51%) patients had nodal disease and 17 (37.7%) patients had disease that was limited to extranodal sites. Five patients had nodal and extranodal disease involvement. The most frequent site of extranodal involvement was the gastrointestinal tract, namely stomach and small and large intestines. Immunohistochemical analysis showed that 41 (97.6%) patients expressed the B-cell marker CD20 (Figure 1B), and all patients expressed CD79α (Figure 1C). All patients tested negative for CD3. Only 5 (11%) patients expressed CD5, and 20 (44.4%) expressed CD10 (Figure 1D). Immunohisochemical staining for BCL2 expression was performed on all patients. Twenty-three (51.1%) patients expressed BCL2 (Figure 1E and Table 1).

Table 1. Cross-tabulation between BCL2 Protein Expression and DLBCL Tumor Site

	Anatomic Site			
BCL2 Protein Expression	Nodal, *n* (%)	Extranodal, *n* (%)	Mixed, *n* (%)	Total
Positive	15 (65.3)[a]	8 (47.1)	0 (0)	23
Negative	8 (34.7)	9 (52.9)	5 (100)	22
Total	23 (100)	17 (100)	5 (100)	45
Significance (*p* value)				0.028[a]

[a]Indicates significance using two-sided Fisher's exact test.

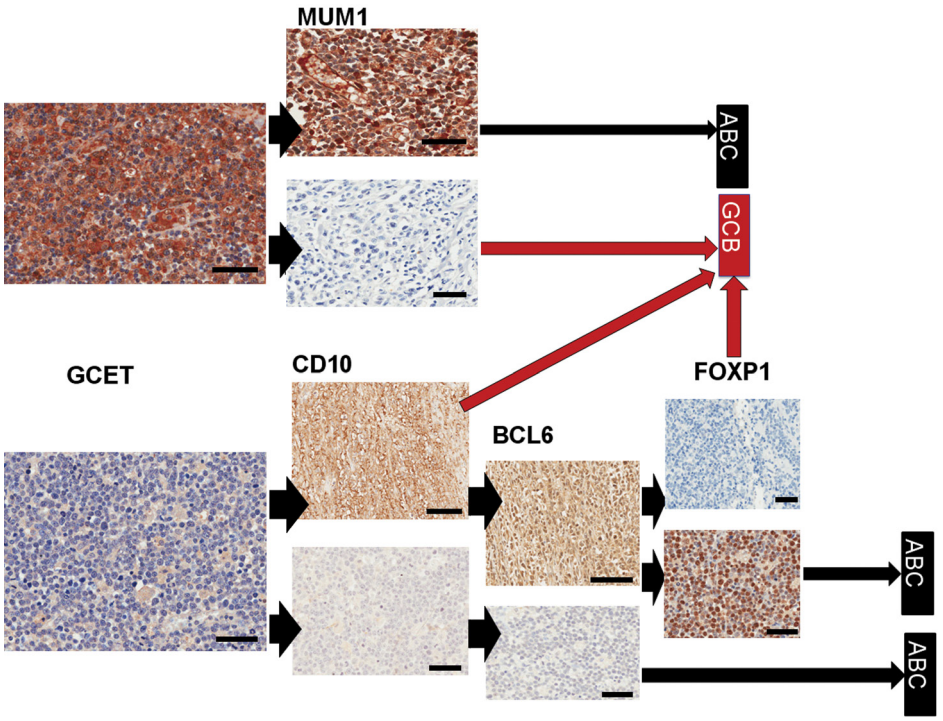

Figure 2. Immunohistochemical staining used in the Choi classification of diffuse large B-cell lymphoma (DLBCL). Sections were first stained for GCET1 protein; if the staining was positive (top left), a parallel section was stained for MUM1 and classified as shown depending on the positivity of MUM1 antibody. If GCET1 staining was negative (bottom left), parallel sections were stained with CD10 as shown. Brown stains indicate positivity and blue hematoxylin counterstains indicate negative expression. Arrowheads show the flow of the data used to generate the algorithm and long arrows the classification reached. GCET, MUM1 lower panel, CD10, BCL6, and FOXP1: bars = 100 µm. MUM1 upper panel and FOXP1 lower panel: bars = 10 µm.

Classifying the DLBCL Using the Choi Algorithm

Recently, Choi et al. (2009) developed a simple immunohistochemical profiling algorithm that uses five antibodies against GCET1, MUM1, CD10, BCL6, and FOXP1 proteins to subclassify DLBCL into subgroups with good prognosis (GCB) and bad prognosis (ABC). The authors showed that the Choi algorithm had 93% concordance with the more sophisticated microarray-based gene expression profiling (Choi et al. 2009). Here, we used the Choi algorithm on 42 of the 45 DLBCL cases (3 cases—1 nodal, 1 extranodal, and 1 mixed—failed subclassification and were excluded from the analysis). Serial and separate sections from each tumor were stained consecutively with the monoclonal antibodies according to the algorithm shown in Figure 2. The classification data of all 42 patients are depicted in Supplementary Table 1. Overall, our data show no statistically significant association between DLBCL site and the ABC/GCB subgroups (Table 2).

Table 2. Association between Choi Classification Using Immunohistochemistry for 5 Protein Markers (GCET1, MUM1, CD10, BCL6, FOXP1) and Tumor Site in 42 DLBCL Patients

	DLBCL Site		
	Nodal, *n* = 22 (52%)	Extranodal, *n* = 16 (38%)	Both, *n* = 4 (10%)
Choi classification, *n*			
ABC[a]	15	6	2
GCB[b]	7	10[c]	2[d]

ABC, activated B-cell–like diffuse large B-cell lymphoma; germinal center B-cell–like diffuse large B-cell lymphoma.
[a]Total *n* = 23 (55%).
[b]Total *n* = 19 (45%).
[c]Nonsignificant ($p = 0.12$) using two-sided χ^2 test (2 × 2 nodal/extranodal vs. ABC/GCB).
[d]Nonsignificance ($p = 0.17$) using two-sided Fisher's exact test (3×2 nodal/extranodal/mixed vs. ABC/GCB).

An Overview of Metaphase CGH Aberrations

Evaluation by CGH was performed on 36 patients who had DNA material suitable for metaphase-CGH analysis. Eighteen patients had disease limited to nodal sites, 13 patients had disease limited to extranodal sites, and 5 patients had extensive disease with nodal and extranodal involvement. All patients showed chromosomal aberrations. The number of aberrations ranged from 1 to 43 with a mean of 14.6. Copy number gains were more frequently observed than losses. The mean ± SD of amplifications was 10.11 ± 7.18, whereas the mean ± SD of deletions was 7.36 ± 5.59. Amplifications were significantly higher than deletions ($p < 0.0001$).

Overall, the most frequent amplifications detected in this study were 7q (61.1%), 11q (52.7%), 1q (47.2%), 7p (38.8%), 12q (38.8%), 17q (38.8%), 20q (36.1%), 1p (30.5%), 9q (30.5%), 17p (30.5%), 3q (27.7%), 16p (27.7%), 3p (25%), 18q (25%), Xq (25%), 22q (22.2%), and Xp (22.2%). The most frequent deletions observed were 4q (33.3%), 9p (33.3%), 6q (30.5%), 4p (27.7%), 13q (27.7%), 18q (27.7%), 5p (25%), 8p (25%), 15q (25%), and 20p (22.2%).

CGH Aberrations in Relation to Anatomic Site

CGH aberrations were then analyzed in relation to the anatomic site of disease involvement. Extranodal lesions had more DNA copy number changes involving multiple chromosomes per patient (mean ± SD = 22.5 ± 11.4) compared with nodal lesions (mean ± SD = 14.4 ± 10.8); however, this difference did not reach statistical significance.

The most frequent chromosomal gains in nodal DLBCL were 1q, 3p, 3q, 5p, 5q, 7p, 7q, 9q, 10q,11q, 12q, 16p, 17p,17q, 18p,18q, and 20q and losses of chromosome arms 1q, 2p, 5p, 7q, 8p, 9p, 11q, 18p, 20p, and Xp (Figure 3A and Figure SF1A). In DLBCL limited to extranodal sites, the most frequent chromosomal gains were 1p, 1q, 3p 7p, 7q, 9p, 9q, 11p, 11q, 12p, 12q, 15q , 16p, 16q, 17p, 17q, 20q, 22q, Xp, and Xq. Chromosomal losses were frequent at 3q, 4p, 4q, 5p, 5q, 6q, 8p, 9p, 13q, 15q, and 18q (Figure 3B and Figure SF1B). The minimal common chromosomal aberrational frequencies are shown in Table 3. Extranodal tumors differed significantly from nodal DLBCLs with regard to amplifications that involved chromosome arms 1p, 7p, 12q, and 22q and chromosome X. Furthermore, deletions of chromosomes 4, 6q, and 18q were significantly more frequent in extranodal lesions compared with nodal lesions (Table 3).

We noted frequent increase in copy number and/or amplification of chromosome 18q, which is the location of the *BCL2* gene, in nodal DLBCL cases compared with extranodal cases (Table 3), although this difference did not reach statistical significance. It was also observed that the frequency of 18q terminal arm deletions was higher in extranodal disease ($n = 6$, 46%) than in nodal disease ($n = 3$, 16.7%). Because BCL2 gene resides on chromosome 18q, we then examined BCL2 gene amplification more closely using FISH and correlated its amplification with the CGH-copy number and BCL2 protein expression data. Using the dual-color t(14;18) FISH Probe, we examined *BCL2* gene amplification and translocation in 36 patients for whom CGH data were available. Translocation (14;18) was detected in only 4 patients (11.1%), and *BCL2* gene amplification was seen in 6 (16.7%) patients. There was significant correlation between BCL2 protein expression and *BCL2* gene amplification (Figure 4). Moreover, the mean count of BCL2 gene copies was 4.47 in nodal lesions compared with 2.63 in extranodal lesions ($p = 0.006$). There was also a highly significant association between chromosome 18q arm copy number increase/amplification and *BCL2* gene amplification detected by FISH (Figure 4). BCL2 protein expression was found to be significantly associated with nodal disease. For example, 15 (65.3%) patients expressing BCL2 had nodal disease compared with 8 (47.1%) patients whose disease was limited to extranodal sites or had extranodal involvement (Table 1). It is worthy of note that 4 of the 5 patients with mixed nodal and extranodal had chromosomal signatures reminiscent of mixed-type of aberrations, although the extranodal sites were analyzed in these cases, possibly suggesting a nodal origin of these tumors (Table ST2).

Narrowing the Genetic Aberrations in Extranodal DLBCL Using High-Resolution 21K BAC Array CGH

In an attempt to verify the CGH data and map the genetic aberrations in extranodal DLBCL more precisely, high-

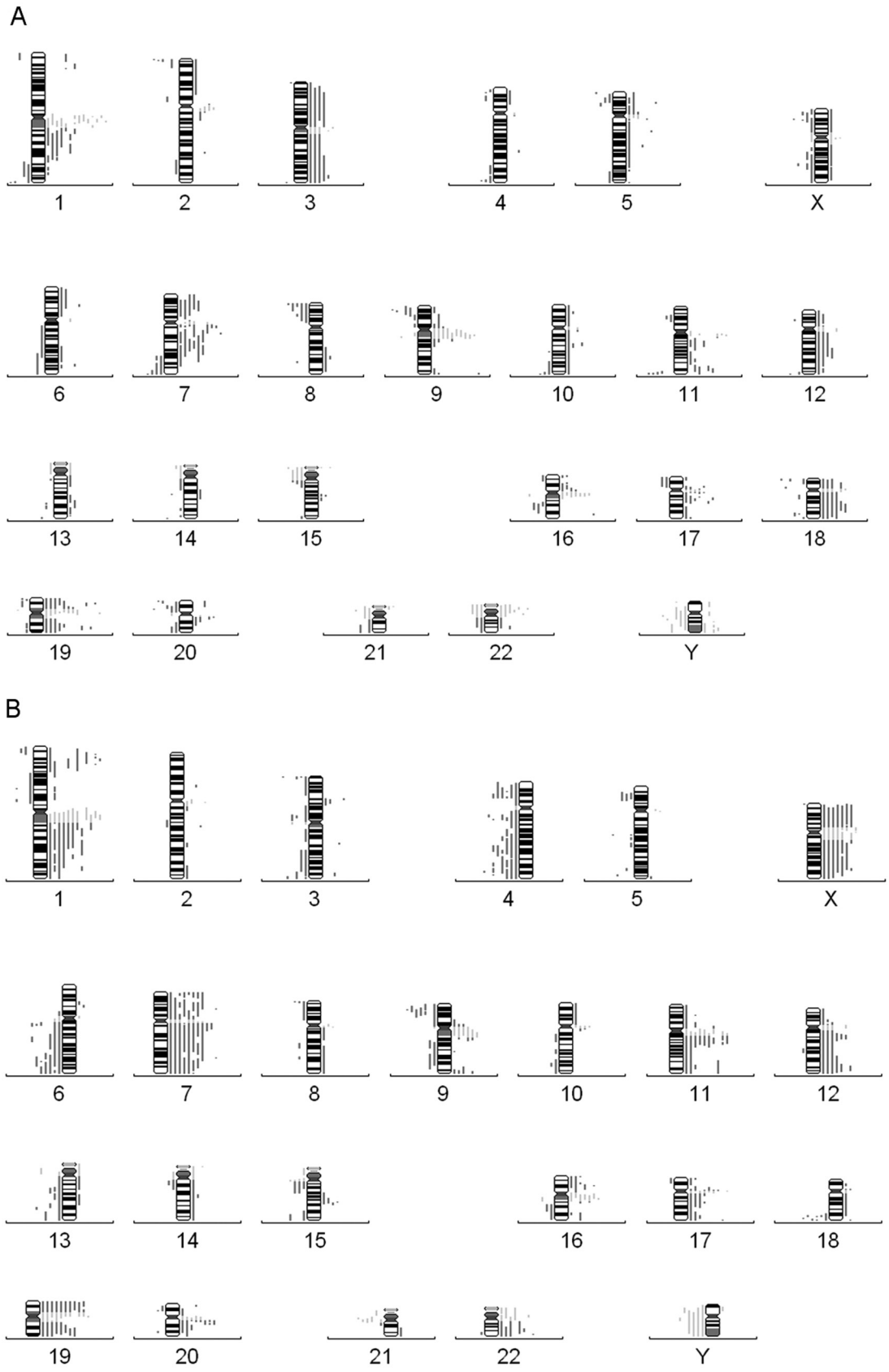

Figure 3. Conventional metaphase comparative genomic hybridization (CGH) profiling of diffuse large B-cell lymphoma (DLBCL). (A) Chromosome profiles from 18 cases of nodal DLBCL. (B) 13 extranodal DLBCL depicting bars on the left of the numbered chromosomal ideograms representing losses and on the right representing gains. Each vertical bar represents a patient. Bar = 1 mm.

Table 3. Metaphase Comparative Genomic Hybridization Analysis of Chromosomal Aberrations in Relation to Anatomic Site

	No. of Patients with Aberrations, *n* = 31					
	Amplifications			Deletions		
Chromosome	Nodal, *n* = 18	Extranodal, *n* = 13	*p* Value	Nodal, *n* = 18	Extranodal, *n* = 13	*p* Value
1p	2 (11.1%)	**7 (53.8%)**	0.016	1 (5.5%)	4 (30.7%)	0.133
1q	7 (38.8%)	9 (69.2%)	0.148	4 (22.2%)	0	0.119
2p	2 (11.1%)	1 (7.6%)	1.000	5 (27.7%)	0	0.058
2q	2 (11.1%)	2 (15.3%)	1.000	1 (5.5%)	1 (7.6%)	1.000
3p	4 (22.2%)	3 (23.07%)	1.000	1 (5.5%)	5 (38.4%)	0.059
3q	5 (27.7%)	2 (15.3%)	0.667	1 (5.5%)	4 (30.7%)	0.133
4p	1 (5.5%)	0	1.000	2 (11.1%)	**6 (46.1%)**	0.042
4q	2 (11.1%)	0	0.496	3 (16.6%)	**8 (61.5%)**	0.020
5p	4 (22.2%)	0	0.119	4 (22.2%)	3 (23.07%)	1.000
5q	4 (22.2%)	1 (7.6%)	0.367	1 (5.5%)	4 (30.7%)	0.133
6p	3 (16.6%)	2 (15.3%)	1.000	0	1 (7.6%)	0.419
6q	2 (11.1%)	0	0.496	2 (11.1%)	**7 (53.8%)**	0.016
7p	5 (27.7%)	**9 (69.2%)**	0.032	0	0	—
7q	10 (55.5%)	11 (84.6)	0.128	4 (22.2%)	0	0.119
8p	0	0	—	5 (27.7%)	3 (23.07%)	1.000
8q	2 (11.1%)	1 (7.6%)	1.000	1 (5.5%)	1 (7.6%)	1.000
9p	3 (16.6%)	3 (23.07%)	1.000	5 (27.7%)	6 (46.1%)	0.449
9q	4 (22.2%)	5 (38.4%)	0.432	0	2 (15.3%)	0.167
10p	2 (11.1%)	1 (7.6%)	1.000	0	0	—
10q	4 (22.2%)	2 (15.3%)	0.683	3 (16.6%)	2 (15.3%)	1.000
11p	0	3 (23.07%)	0.063	2 (11.1%)	0	0.496
11q	7 (38.8%)	10 (76.9%)	0.066	4 (22.2%)	0	0.119
12p	2 (11.1%)	3 (23.07%)	0.625	1 (5.5%)	0	1.000
12q	4 (22.2%)	7 (53.8%)	0.127	2 (11.1%)	1 (7.6%)	1.000
12q24.21-24.31	2 (11.1%)	**6 (46.1%)**	0.042	0	0	—
13q	2 (11.1%)	1 (7.6%)	1.000	3 (16.6%)	5 (38.4%)	0.228
14q	1 (5.5%)	2 (15.3%)	0.557	3 (16.6%)	2 (15.3%)	1.000
15q	2 (11.1%)	4 (30.7%)	0.358	3 (16.6%)	4 (30.7%)	0.413
16p	4 (22.2%)	5 (38.4%)	0.432	1 (5.5%)	0	1.000
16q	1 (5.5%)	3 (23.07%)	0.283	3 (16.6%)	2 (15.3%)	1.000
17p	4 (22.2%)	6 (46.1%)	0.246	2 (11.1%)	1 (7.6%)	1.000
17q	7 (38.8%)	5 (38.4%)	1.000	0	0	—
18p	4 (22.2%)	2 (15.3%)	0.683	4 (22.2%)	0	0.119
18q	6 (33.3%)	2 (15.3%)	0.412	3 (16.6%)	6 (46.1%)	0.114
18q22.3-23	4 (22.2%)	1 (7.6%)	0.367	1 (5.5%)	**6 (46.1%)**	0.012
20p	1 (5.5%)	2 (15.3%)	0.557	6 (33.3%)	2 (15.3%)	0.412
20q	4 (22.2%)	8 (61.5%)	0.059	2 (11.1%)	1 (7.6%)	1.000
21q	0	1 (7.6%)	0.419	2 (11.1%)	1 (7.6%)	1.000
22q	2 (11.1%)	**6 (46.1%)**	0.042	2 (11.1%)	1 (7.6%)	1.000
Xp	1 (5.5%)	**7 (53.8%)**	0.004	4 (22.2%)	1 (7.6%)	0.367
Xq	1 (5.5%)	**7 (53.8%)**	0.004	3 (16.6%)	0	0.245

Boldface numbers indicate significance using two-sided Fisher's exact test.

resolution 21K BAC arrays were used to localize genomic alterations in an independent cohort of 12 additional extranodal DLBCL tumors. Table 4 summarizes the most frequent aberrations identified in these patients. Interestingly, the genetic signature that discriminated extranodal from nodal tumors, which we identified in the first cohort using metaphase CGH, was highly represented in this independent extranodal cohort (Figure SF2). For example, gain of

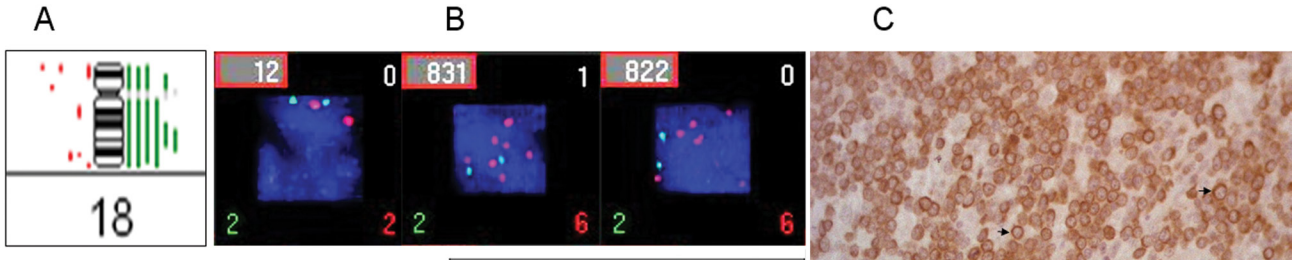

D

		BCL2 gene amplification (FISH) Positive	Negative
BCL2 protein expression	Positive	6*	0
	Negative	13	15
	*p=0.024 using two-sided Fisher's exact test		
Ch 18q CGH amplification	Positive	4*	4
	Negative	2	23
	*p=0.02 using two-sided Fisher's exact test		

Figure 4. 18q and BCL2 are increased in copy number in nodal diffuse large B-cell lymphoma (DLBCL). (A) Metaphase comparative genomic hybridization (CGH) of chromosome 18 from 18 patients with nodal DLBCL showing six green vertical bars on the right of the ideogram and indicating increase in copy number. (B) Fluorescent in situ hybridization of dual color dual fusion translocation probe t(14;18)(q32;q21) from three representative patients: a control on the left and two patients with nodal DLBCL showing increased red signals localized to chromosome 18q21 and 2 green signals for chromosome 14q32. (C) Shows positive immunohistochemistry of a nodal DLBCL patient for BCL2 protein with arrows pointing to membranous BCL2 protein staining. (D) Correlation between fluorescence in situ hybridization (FISH), CGH, and BCL2 expression in DLBCL patients regardless of site. Bar = 100 μm.

X chromosome was found in 25–42% of patients, gains of chromosomal arms 12q24.21-12q24.31 and 22q13.2 were found in 25% of patients, and loss of chromosome 4p15.32-4p15.1 and 18q22.3-18q23 was identified in 25–33% of tumors (Table 4 and Figure SF3). Side-by-side comparisons of the chromosomal aberrations identified in the two separate extranodal cohorts and possible genes localized to these areas are shown in Figure 5. It is worthy of note that the aCGH data showed similar tendencies for genetic heterogeneity between samples. Figure 6 shows that gastrointestinal/thyroid/bone DLBCLs as a group harbored significantly more losses at chromosome arm 5p15.33 and gains at chromosome arm Xp11.3 than head/oral DLBCLs (p = 0.02 using ANOVA). These data indicate that even within extranodal tumors, there appear to be significant chromosome imbalances that may be site dependent.

Discussion

In this study we showed that at the genomic level, nodal and extranodal DLBCL tumors differ significantly. We identified a genetic signature exemplified by gain at chromosome arms 1p36.12-1p35.2, 12q24.21-12q24.31, and 22q13.2 and chromosome X and loss of chromosomal regions 4p15.32-4p15.1 and 18q22.3-18q23 that is commonly present in extranodal compared with nodal DLBCLs. Moreover, nodal DLBCL tumors have elevated expression level of BCL2 protein seemingly arising from increased copy number/amplification at 18q chromosome arm. We found that gains were more frequent than losses, with the most frequent CGH aberrations in DLBCL being gains involving chromosomes 1, 3, 7, 11, 12, 17, 18, 20, and X and the most frequent losses involving chromosomes 4, 5, 6, 8, 9, 13, 15, and 18, most of which are in agreement with previously reported studies (Monni et al. 1997; Wilkens et al. 1998; Berglund et al. 2002). Several studies have shown that DLBCL is a disease that involves multiple inconsistent CGH aberrations (Monni et al. 1997; Wilkens et al. 1998; Berglund et al. 2002). Such multiple chromosome abnormalities may indicate that DLBCL is a lesion that is pathogenetically initiated by multiple and probably sequential genetic lesions.

Our data pertaining to the extranodal genetic signature are more difficult to compare with current studies in the literature because most, if not all, have focused the analysis on DLBCL without elaborating on the sites of involvement or have focused on primary nodal tumors or nodal tumors with extranodal involvement. Nevertheless, DNA copy analysis in DLBCL with the use of CGH has been an important source of data concerning the nature and frequency of CGH aberrations in this common type of NHL (Monni et al. 1996; Gascoyne et al. 1997; Wilkens et al. 1998; Berglund et al. 2002; Bea et al.

Table 4. Most Frequent Chromosomal Regions with Imbalances Identified Using Array Comparative Genomic Hybridization in 12 Patients with Extranodal Diffuse Large B-cell Lymphoma

Region	Region Length	Cytoband Location	Event	Genes	miRNAs	Frequency, %	% of CNV Overlap
chr19:0-24,420,506	24420506	p13.3-p12	CN gain	630	19	58.3	52.2
chr5:3,803,270-5,386,661	1583391	p15.33-p15.32	CN loss	2	0	50.0	28.3
chr7:15,280,377-18,783,707	3503330	p21.1	CN loss	13	1	50.0	47.5
chr11:15,064,663-16,102,411	1037748	p15.2-p15.1	CN loss	2	0	41.7	1.8
chr11:17,773,600-18,436,773	663173	p15.1	CN loss	15	0	41.7	5.9
chr11:60,512,821-63,918,223	3405402	q12.2-q13.1	CN gain	118	3	41.7	46.9
chr2:4,555,846-7,626,996	3071150	p25.2-p25.1	CN loss	6	0	41.7	17.1
chr5:10,804,333-13,772,767	2968434	p15.2	CN loss	3	0	41.7	34.4
chr7:73,945,120-76,028,338	2083218	q11.23	CN gain	36	0	41.7	100.0
chrX:50,886,737-55,726,646	**4839909**	**p11.22-p11.21**	**CN gain**	**84**	**2**	**41.7**	**62.9**
chrX:69,420,195-70,728,377	**1308182**	**q13.1**	**CN gain**	**21**	**0**	**41.7**	**89.5**
chr10:3,496,279-4,818,106	1321827	p15.2-p15.1	CN loss	3	0	33.3	4.8
chr3:50,741,118-51,772,505	1031387	p21.31-p21.1	CN gain	7	0	33.3	12.2
chr4:27,781,570-33,954,303	**6172733**	**p15.2-p15.1**	**CN loss**	**1**	**0**	**33.3**	**26.3**
chr8:99,025,182-102,051,182	3026000	q22.1-q22.3	CN gain	23	3	33.3	29.3
chrX:72,215,421-76,514,933	**4299512**	**q13.2-q21.1**	**CN gain**	**25**	**6**	**33.3**	**16.9**
chr1:202,572,242-205,707,496	3135254	q32.1-q32.2	CN loss	50	1	25.0	18.0
chr1:211,518,057-213,522,592	2004535	q32.3-q41	CN loss	6	0	25.0	0.6
chr10:128,685,991-134,906,603	6220612	q26.2-q26.3	CN loss	26	0	25.0	48.0
chr11:131,053,908-132,949,322	1895414	q25	CN loss	2	0	25.0	44.4
chr11:132,949,322-134,452,384	1503062	q25	CN gain	12	0	25.0	53.5
chr11:47,645,154-50,272,727	2627573	p11.2-p11.12	CN gain	16	0	25.0	71.3
chr12:119,620,653-121,772,270	**2151617**	**q24.31**	**CN gain**	**36**	**0**	**25.0**	**26.1**
chr13:18,993,169-20,772,638	1779469	q12.11	CN gain	17	0	25.0	58.8
chr14:77,458,101-78,443,996	985895	q24.3-q31.1	CN loss	2	0	25.0	42.5
chr14:82,029,831-83,788,141	1758310	q31.1-q31.2	CN loss	0	0	25.0	26.4
chr14:96,454,283-98,632,766	2178483	q32.2	CN loss	2	0	25.0	13.9
chr18:70,331,151-72,136,349	**1805198**	**q22.3-q23**	**CN loss**	**7**	**0**	**25.0**	**8.4**
chr2:107,639,140-109,124,717	1485577	q12.3-q13	CN gain	13	0	25.0	53.4
chr2:163,026,864-165,253,762	2226898	q24.2-q24.3	CN loss	4	0	25.0	8.4
chr20:6,250,059-11,472,027	5221968	p12.3-p12.2	CN loss	12	0	25.0	32.6
chr22:39,989,292-42,100,036	2110744	q13.2	CN gain	47	1	25.0	41.8
chr3:106,133,787-107,787,489	1653702	q13.11	CN loss	2	0	25.0	30.8
chr4:19,046,051-22,412,754	**3366703**	**p15.31**	**CN loss**	**7**	**1**	**25.0**	**38.6**
chr5:161,486,068-162,710,460	1224392	q34	CN gain	1	0	25.0	5.8
chr5:176,474,585-179,601,901	3127316	q35.2-q35.3	CN gain	56	2	25.0	44.6
chr5:20,648,414-24,667,707	4019293	p14.3-p14.2	CN loss	5	0	25.0	33.7
chr5:43,354,667-46,437,323	3082656	p12-p11	CN gain	8	0	25.0	25.9
chr6:40,000,579-41,899,173	1898594	p21.2-p21.1	CN loss	25	0	25.0	9.1
chr8:142,762,585-146,274,826	3512241	q24.3	CN gain	103	5	25.0	59.4
chr9:117,824,871-120,178,394	2353523	q33.1	CN loss	5	0	25.0	15.2
chrX:93,832,178-132,744,538	**38912360**	**q21.33-q26.2**	**CN gain**	**279**	**10**	**25.0**	**27.5**

Boldface regions identify extranodal DLBCL genetic signature. CN, Copy number; CNV, Copy number variation; miRNA, Micro-RNA.

2005; Tagawa et al. 2005; Chen et al. 2006; Xia et al. 2006). These studies have identified aberrations that included DNA gains and losses involving various chromosomes. Furthermore, data on BCL2 protein expression in DLBCL were correlated with treatment outcome and survival data in various reports (Kramer et al. 1996; Beã et al. 2004).

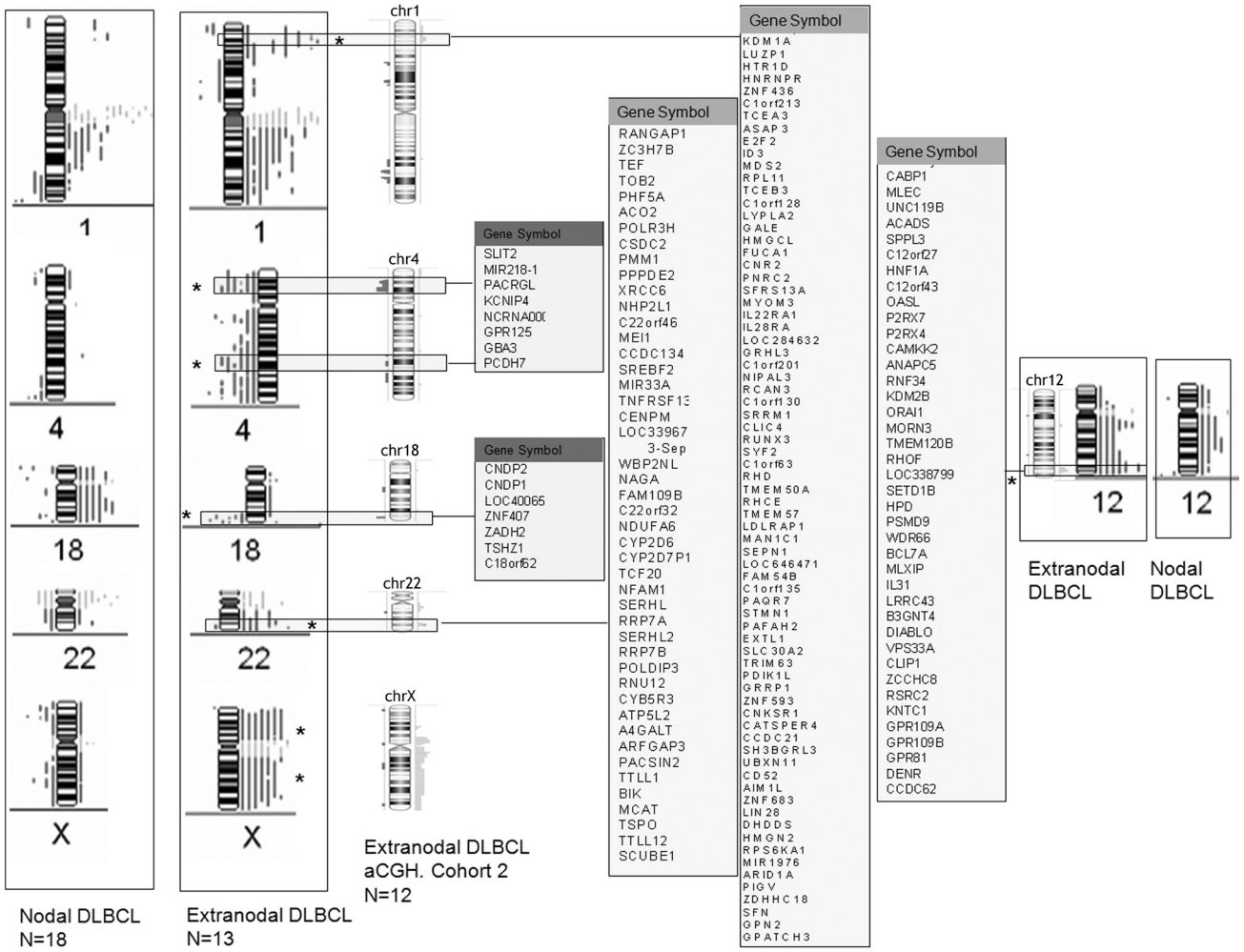

Figure 5. Side-by-side comparison of metaphase and array comparative genomic hybridization (aCGH) data of DLBCL tumors focused on the extranodal genetic signature. The middle panels represent genes localized to the specified areas. Asterisks represent significance at $p < 0.05$.

BCL2 protein inhibits apoptosis and is present at low levels in normal germinal centers. However, it is overexpressed in some NHL cells that have a t(14;18) translocation. Its overexpression, as detected immunohistochemically, has been shown in previous studies to be an independent marker of poor prognosis in patients with DLBCL (Kramer et al. 1996; Rantanen et al. 2001; Iqbal et al. 2006).

The current study demonstrates interesting aspects of BCL2 protein expression and CGH alterations in relation to the anatomic site of the disease. The results of our study show that BCL2 protein expression was more common in nodal compared with extranodal DLBCL patients. Furthermore, there was a good concordance between the overexpression of the BCL2 oncoprotein and the increased BCL2 FISH signal amplification in nodal lesions. These findings support the fact that overexpression of BCL2 oncoprotein is a result of BCL2 gene amplification and chromosome 18q increased copy number, a finding that supports the hypothesis of others who proposed that the level of BCL2 protein expression may be increased in neoplastic cells of lymphoproliferative disorders without BCL2 gene rearrangement (Hermine et al.1996, Monni et al. 1997 Rantanen et al. 2001 and Berglund et al. 2002). In addition, our metaphase CGH results showed that nodal lesions have more frequent amplifications of chromosome 18 (18q) than extranodal lesions. However, although this difference was not statistically significant, the matched BCL2 protein overexpression together with the BCL2 FISH signal amplification and the CGH aberrations involving chromosome 18 might collectively indicate that site-specific mechanism plays a role in the pathogenesis and selection of nodal vs extranodal DLBCL. Furthermore, although the relation between BCL2 overexpression and BCL2 gene amplification was previously demonstrated, these findings have not

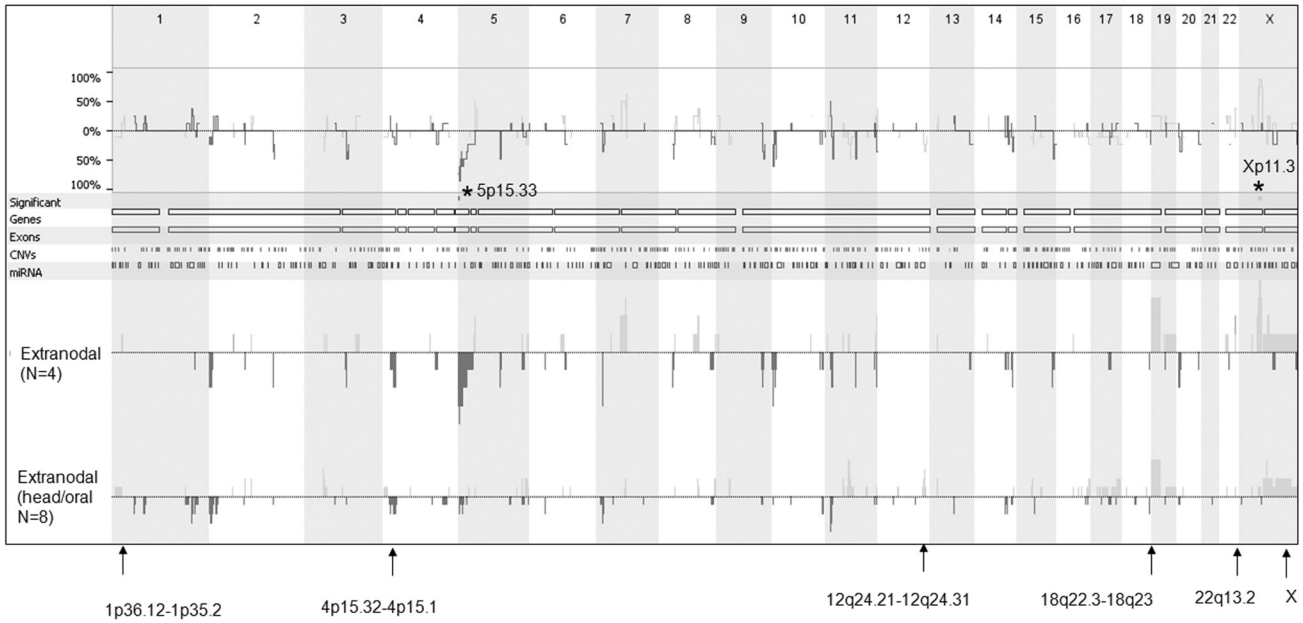

Figure 6. Array comparative genomic hybridization (aCGH) showing genomic differences between 4 extranodal DLBCLs localized to intestine (n = 2), thyroid (n = 1), and bone (n = 1) as a group termed extranodal and a second group of extranodal DLBCL tumors localized to head/oral cavity (n = 8). Top panel is a frequency plot that summarizes the differences in aberrations obtained from the two groups. The chromosome numbers are shown at the top of the figure. The lower panel indicates genetic aberrations in each group labeled on the left. Lines and bars below the 0-$\log_2$ ratio indicate deletions and ones above it indicate amplifications. Asterisks represent significance at $p < 0.05$ using ANOVA statistics. Arrows point to the specified chromosomal extranodal signature.

been previously correlated with the anatomic site of DLBCL (Hermine et al. 1996; Monni et al. 1997; Rantanen et al. 2001; Berglund et al. 2002).

We were also able to identify previously unreported aberrations of amplifications involving chromosome 1 (1p and 1q) and deletions involving chromosome 4 being more frequent in extranodal compared with nodal disease. These findings may be related to the site-specific nature of DLBCL pathogenesis and to its predominant site of involvement. In DLBCL, Chen and colleagues (2006) have identified 55 commonly gained/deleted regions that correlated with overall survival, using 1- to 2-Mbp and 2- to 4-Mbp resolution BAC arrays, of which losses of chromosomes 2 (2.4-4.1 Mbp) and 16 (33.8-35.6 Mbp) were found to be prognostic indicators of poor survival and loss of chromosome 1 (78.2-79.1 Mbp) was predictive of good outcome.

In the current study, we used high-resolution 21K tiling-BAC array CGH on 12 extranodal DLBCL patients and thus were able to narrow down regions that might harbor important genes involved in the pathogenesis of extranodal DLBCL. The utility of this comprehensive assay was made evident by the detection and localization of frequent genomic gains and/or losses involving chromosomes 2, 5, 7, 11, and 19; however, the region lengths, the cytoband locations, and the number of involved genes that were identified in the current study were different from those reported by Chen and colleagues, possibly because our patients on whom aCGH was performed all had extranodal DLBCL lesions. Furthermore, Hussain et al. (forthcoming) showed that the X-linked inhibitor of apoptosis protein (XIAP) was overexpressed in 55% of their DLBCL patients. Their findings could be related to increased copy number and amplification that were detected in chromosome X in 42% of our extranodal DLBCL patients.

Previous reports have shown that the expression of CD5, as a biological marker, appeared to be associated with high-risk International Prognostic Index (IPI), hence indicating that de novo $CD5^+$ DLBCL is a highly aggressive subtype (Karnan et al. 2004; Tagawa et al. 2004). However, the small number of $CD5^+$ DLBCL patients in our study did not allow us to analyze the distribution of CGH aberration among this subgroup. Nevertheless, using the Choi classification (Choi et al. 2009) on our DLBCL patients indicated two important ramifications. First, the ABC subgroup constituted more than half of the DLBCLs in Kuwait, which may explain the aggressive disease our clinicians observe locally. Second, the genomic differences observed between nodal and extranodal DLBCLs appear to be genuinely related to site and not ABC/GCB subclassification. Therefore, identifying separate genetic signatures for nodal and extranodal DLBCL may have diagnostic and/or prognostic implications in that when a nodal genetic signature is

found in an extranodal site, it may guide in the search for nodal involvement and vice versa.

In summary, DLBCL is a heterogeneous group of diseases as evident by its diverse DNA aberrations that were detected by CGH. Gains were more frequent than losses. There were differences between nodal and extranodal DLBCL patients in relation to BCL2 overexpression, BCL2 gene amplification, and genetic aberrations. However, this study is retrospective, and we did not correlate our findings with survival data; therefore, a larger and prospective study is needed to establish the significance of these results. Moreover, we realize that using DNA extracted from FFPE tissues may have represented a limitation in our study; future studies may benefit from using DNA extracted from frozen tissue in a separate cohort of patients.

Acknowledgments

We thank the Canadian Embassy in Kuwait as well as the Terry Fox Foundation for their support in pursuing this project (Project Grant Nos. TFF/4/00 and TFF/01/07) in Kuwait and providing the necessary funding for this research. We also extend our appreciation to Dr. Rosemary Makar for her effort to get this study started and to the competent technologists Mrs. Sindhu Jacob and Diana Thomas for their tremendous effort. The proteomics and microarray analysis were performed in the Research Core Facility of the Health Sciences Center supported by projects GM 01/01 and GM 01/05.

Declaration of Conflicting Interests

The author(s) declared no potential conflicts of interest with respect to the authorship and publication of this article.

Funding

The author(s) received no financial support for the research and authorship of this article.

References

Alizadeh AA, Eisen MB, Davis RE, Ma C, Lossos IS, Rosenwald A, Boldrick JC, Sabet H, Tran T, Yu X, Powell JI, et al. Distinct types of diffuse large B-cell lymphoma identified by gene expression profiling. Nature 2000;403(6769):503–11.

Al-Mulla F, Behbehani AI, Bitar MS, Varadharaj G, Going JJ. Genetic profiling of stage I and II colorectal cancer may predict metastatic relapse. Mod Pathol 2006;19(5):648–58.

Ameen R, Sajnani KP, Albassami A, Refaat S. Frequencies of non-Hodgkin's lymphoma subtypes in Kuwait: comparisons between different ethnic groups. Ann Hematol 2010;89:179–84.

Beã S, Colomo L, Lãpez-Guillermo A, Salaverria I, Puig X, Pinyol M, Rives S, Montserrat E, Campo E. Clinicopathologic significance and prognostic value of chromosomal imbalances in diffuse large B-cell lymphomas. J Clin Oncol 2004;22(17):3498–506.

Bea S, Zettl A, Wright G, Salaverria I, Jehn P, Moreno V, Burek C, Ott G, Puig X, Yang L, et al.; Lymphoma/Leukemia Molecular Profiling Project. Diffuse large B-cell lymphoma subgroups have distinct genetic profiles that influence tumor biology and improve gene-expression-based survival prediction. Blood 2005;106(9):3183–90.

Berglund M, Enblad G, Flordal E, Lui WO, Backlin C, Thunberg U, Sundstrã MC, Roos G, Allander SV, Erlanson M, et al. Chromosomal imbalances in diffuse large B-cell lymphoma detected by comparative genomic hybridization. Mod Pathol 2002;15(8):807–16.

Chen W, Houldsworth J, Olshen AB, Nanjangud G, Chaganti S, Venkatraman ES, Halaas J, Teruya-Feldstein J, Zelenetz AD, Chaganti RS. Array comparative genomic hybridization reveals genomic copy number changes associated with outcome in diffuse large B-cell lymphomas. Blood 2006;107(6):2477–85.

Choi W, Weisenburger D, Greiner T, Piris M, Banham A, Delabie J, Braziel R, Geng H, Iqbal J, Lenz G, et al. A new immunostain algorithm classifies diffuse large B-cell lymphoma into molecular subtypes with high accuracy. Clin Cancer Res 2009;15(17):5494–502.

Gascoyne RD, Adomat SA, Krajewski S, Krajewska M, Horsman DE, Tolcher AW, O'Reilly SE, Hoskins P, Coldman AJ, Reed JC, et al. Prognostic significance of Bcl-2 protein expression and Bcl-2 gene rearrangement in diffuse aggressive non-Hodgkin's lymphoma. Blood 1997;90(1):244–51.

Hermine O, Haioun C, Lepage E, d'Agay MF, Briere J, Lavignac C, Fillet G, Salles G, Marolleau JP, Diebold J, et al. Prognostic significance of bcl-2 protein expression in aggressive non-Hodgkin's lymphoma. Groupe d'Etude des Lymphomes de l'Adulte (GELA). Blood 1996;87(1):265–72.

Hussain AR, Uddin S, Ahmed M, Bu R, Ahmed SO, Abubaker J, Sultana M, Ajarim D, Al-Dayel F, Bavi PP, et al. Prognostic significance of XIAP expression in DLBCL and effect of its inhibition on AKT signaling. J Pathol. Forthcoming.

Iqbal J, Neppalli VT, Wright G, Dave BJ, Horsman DE, Rosenwald A, Lynch J, Hans CP, Weisenburger DD, Greiner TC, et al. BCL2 expression is a prognostic marker for the activated B-cell-like type of diffuse large B-cell lymphoma. J Clin Oncol 2006;24(6):961–8.

Karnan S, Tagawa H, Suzuki R, Suguro M, Yamaguchi M, Okamoto M, Morishima Y, Nakamura S, Seto M. Analysis of chromosomal imbalances in de novo CD5-positive diffuse large-B-cell lymphoma detected by comparative genomic hybridization. Genes Chromosomes Cancer 2004;39(1):77–81.

Kramer MH, Hermans J, Parker J, Krol AD, Kluin-Nelemans JC, Haak HL, van Groningen K, van Krieken JH, Jong D de, Kluin PM. Clinical significance of bcl2 and p53 protein expression in diffuse large B-cell lymphoma: a population-based study. J Clin Oncol 1996;14(7):2131–8.

Lawrie CH, Soneji S, Marafioti T, Cooper CD, Palazzo S, Paterson JC, Cattan H, Enver T, Mager R, Boultwood J, et al. MicroRNA expression distinguishes between germinal center B cell-like and activated B cell-like subtypes of diffuse large B cell lymphoma. Int J Cancer 2007; 121(5):1156–61.

Monni O, Joensuu H, Franssila K, Knuutila S. DNA copy number changes in diffuse large B-cell lymphoma—comparative genomic hybridization study. Blood 1996;87(12):5269–78.

Monni O, Joensuu H, Franssila K, Klefstrom J, Alitalo K, Knuutila S. BCL2 overexpression associated with chromosomal amplification in diffuse large B-cell lymphoma. Blood 1997;90(3):1168–74.

Rantanen S, Monni O, Joensuu H, Franssila K, Knuutila S. Causes and consequences of BCL2 overexpression in diffuse large B-cell lymphoma. Leuk Lymphoma 2001;42(5):1089–98.

Rosenwald A, Wright G, Chan WC, et al. The Use of molecular profiling to predict survival after chemotherapy for diffuse large B-cell lymphoma. N Engl J Med 2002;364:1937–47.

Rosenwald A, Staudt LM. Gene expression profiling of diffuse large B-cell lymphoma. Leuk Lymphoma. 2003;44 Suppl 3:S41–7.

Savage KJ, Monti S, Kutok JL, Cattoretti G, Neuberg D, de Leval L, Kurtin P, Dal Cin P, Ladd C, Feuerhake F, et al. The molecular signature of mediastinal large B-cell lymphoma differs from that of other diffuse large B-cell lymphomas and shares features with classical Hodgkin lymphoma. Blood 2003;102(12):3871–9.

Tagawa H, Suguro M, Tsuzuki S, Matsuo K, Karnan S, Ohshima K, Okamoto M, Morishima Y, Nakamura S, Seto M. Comparison of genome profiles for identification of distinct subgroups of diffuse large B-cell lymphoma. Blood 2005;106(5):1770–7.

Tagawa H, Tsuzuki S, Suzuki R, Karnan S, Ota A, Kameoka Y, Suguro M, Matsuo K, Yamaguchi M, Okamoto M, et al. Genome-wide array-based comparative genomic hybridization of diffuse large B-cell lymphoma: comparison between CD5-positive and CD5-negative cases. Cancer Res 2004;64(17):5948–55.

Wilkens L, Tchinda J, Burkhardt D, Nolte M, Werner M, Georgii A. Analysis of hematologic diseases using conventional karyotyping, fluorescence in situ hybridization (FISH), and comparative genomic hybridization (CGH). Hum Pathol 1998;29(8):833–9.

Wright G, Tan B, Rosenwald A, Hurt EH, Wiestner A, Staudt LM. A gene expression-based method to diagnose clinically distinct subgroups of diffuse large B-cell lymphoma. Proc Natl Acad Sci U S A 2003;329:987–94.

Xia HL, Chen LJ, Chen B, Jin XL, Chen SJ. The molecular cytogenetic aberration analyzed by comparative genomic hybridization and its significance in diffuse large B-cell lymphoma. Zhonghua Yi Xue Yi Chuan Xue Za Zhi 2006;23(1):12–5.